

Article

# Lighting Implications of Urban Mitigation Strategies through Cool Pavements: Energy Savings and Visual Comfort

Giuseppe Rossi <sup>1</sup>, Paola Iacomussi <sup>1,\*</sup>  and Michele Zinzi <sup>2</sup>

<sup>1</sup> INRIM, Istituto Nazionale di Ricerca Metrologica, Strada delle Cacce 91, 10135 Torino, Italy; g.rossi@inrim.it

<sup>2</sup> ENEA, National Agency for New Technologies, Energy and Sustainable Economic Development, Via Anguillarese 301, 00123 Rome, Italy; michele.zinzi@enea.it

\* Correspondence: p.iacomussi@inrim.it; Tel.: +39-011-3919226

Received: 31 January 2018; Accepted: 26 March 2018; Published: 7 April 2018



**Abstract:** Cool materials with higher solar reflectance compared with conventional materials of the same color are widely used to maintain cooler urban fabrics when exposed to solar irradiation and to mitigate the Urban Heat Island (UHI). Photo-catalytic coatings are also useful to reduce air pollutants. Many studies related to these topics have been carried out during the past few years, although the lighting implication of reflective coatings have hardly been explored. To investigate these aspects, reflective coatings were applied on portions of a road and intensely analyzed in a laboratory and on the field. The applied cool coatings were found to have much higher solar and lighting reflectance than the existing road, which lead to lower surface temperatures up to 9 °C. Non-significant variations of chromaticity coordinates were measured under different lighting conditions. However, these materials showed a relevant variation of directional properties depending on the lighting and observation conditions with respect to conventional pavements. The optical behavior of these materials affects the uniformity of visions for drivers and requires ad-hoc installation of light sources. On the other hand, potential energy savings of up to 75% were calculated for the artificial lighting of a reference road.

**Keywords:** cool pavements; road lighting; urban heat island; road surface; material characterization; luminance coefficient; energy savings; Euramet; EMPIR 16NRM02

## 1. Introduction

Urban Heat Island (UHI) and urban overheating are two major environmental hazards arising from the combined force of climate change and unregulated growth of cities. The UHI is defined as the increase in urban temperatures in proportion to those of the countryside surrounding the city. The phenomenon is complex and there is still no complete explanation. However, the main causes are: the reduction of permeable surfaces, the use of high solar absorptive construction materials, the anthropogenic heat generated by energy uses in the civil and transport sectors and the urban texture geometry that creates favorable conditions for heat trapping and low heat release [1–3].

Extensive studies on the UHI phenomenon and associated mitigation strategies were started several decades ago [1–5], which have intensified in the new millennium due to experiences documented at all latitudes, which has been summarized in literature review studies [6–9]. The increase in urban ambient temperatures has been documented through pluriannual observations for many US and European cities [8,9] as result of the combined effect of global warming and urban heat islands. According to vast literature surveys carried out in recent years, it was found out that UHI intensity reached 15 °C in the most sever conditions [6].

This trend shows that these serious urban climate hazards have not been adequately tackled, especially considering that it has a relevant impact at the energy, environmental and social levels, as widely documented in several exemplary studies [10–15]. On the contrary, several mitigation strategies and technologies are available to counter this phenomenon. Some of these are consolidated enough to be considered as a trademark for vernacular architecture and urbanism in several areas of the world. Such solutions can be gathered in four large categories: urban and building greenery; natural and artificial water bodies; urban shading; and cool construction materials for pavements and buildings. The impact of such solutions, each separately and/or combined, has been proven in many studies. Exhaustive reviews have been already conducted [7,16–18].

The applications of white and light-colored materials for buildings have been carried out for centuries, becoming a trademark of vernacular architecture in the Mediterranean region [19]. This ancient concept gained attention with the so-called cool materials, which are products with higher solar reflectance compared with conventional materials of the same color. Due to this, they are able to remain cooler under solar irradiation. A higher solar reflectance results in lower material surface temperature under the sun, subsequently resulting in less heat released to the outdoor and indoor environments by convection and radiation. White and light-colored materials have the highest potential for thermal mitigation. Despite the effort exerted in maximizing the solar reflectance in the near-infrared region in the past few years so that even darker color could achieve good performances, several studies have demonstrated the stronger mitigation benefits of high albedo materials [20–23]. Generally, cool materials also have high thermal emissivity, although the impact of this property on UHI is less than that of their reflectance [24]. Comprehensive reviews about cool pavements and the impact on urban climate can be found in previous studies [25–28].

The potential impact of high solar reflectance materials in mitigating the urban environment was investigated in the past few years. Several studies are based on the preliminary monitoring of urban area and assessment of potential mitigation through Computational Fluid Dynamic (CFD) simulations. An application covering 25,000 m<sup>2</sup> was carried out in Tirana, Albania, where existing concrete and asphalt pavements were upgraded with cool paints. The albedo increased from 0.2 to above 0.65, with a 2.1-K predicted decrease in the peak ambient temperature [29]. A similar application was carried out in Athens, Greece, where the existing pavements were replaced with different products with albedo ranging between 0.35 and 0.78. The peak temperature reduction was estimated as being 1.2–2 K on average [30]. A relevant application was carried out in Putrajaya, Malaysia, in which a 420,000 m<sup>2</sup> urban area was upgraded with greenery and pavements, with 0.8 albedo. The ambient temperature reduction was estimated to be 1.5 K, of which only 0.1 K seemed to be related to the use reflective materials [31].

It can be inferred that a considerable amount of work has been done on the thermal aspects, although there has been little evidence related to environmental lighting conditions and on the lighting associated impact. The latter refers to artificial lighting energy savings as well as to glare and visual discomfort risks arising from materials with high reflectance in the visible range and enhanced directional properties [32].

Cool materials, which are based on photo-catalytic solutions with titanium dioxide or with dispersed silicates, are often used for road surfaces in urban zones due to their self-cleaning capability and their capability to reduce harmful substances (pollutants) in air. These products are applied on existing roads by spray guns using standard methods without considering their influence on the optical properties of the road surface and changes in lighting conditions and night/day vision.

The knowledge of the road surface luminance coefficient is important for the optimization of the energy performances of the lighting installations [33], glare evaluation [34] and improvement of safety, comfort during the night and energy savings. For example, this could occur through LED adaptive lighting systems (smart cities) [35]. The introduction of the European standards of energy performance indicators [33] and correlated requirements asks for improved optimization in the design of luminaries and selection of their luminous intensity distribution in addition to the installation layout and optical

characteristics of the road surface. The use of brighter road surfaces can reduce the UHI effects during the day and improve energy saving and traffic safety during the night.

This study investigates the implications of applying high reflective coatings in design and performances of road lighting installations when these coatings are used in urban environments to rehabilitate existing pavements and road surfaces for thermal mitigation. For this purpose, cool coatings were tested for visual comfort and energy lighting assessment. To fully understand behavior and performances of such products, the following process was implemented:

- application of cool coatings in the real urban environment;
- optical, luminous and thermal characterization with laboratory measurements;
- luminous and thermal measurements in real urban conditions;
- simulation of artificial lighting energy saving and power performances of a standard road lighting installations.

All the analyses were carried out by considering reference asphalt pavements and cool pavements in order to compare differences in properties and performances for lighting related issues.

## 2. Materials and Methods

### 2.1. Theoretical Background

This section is dedicated to recall the basic theoretical concepts related to the directional properties of construction materials and the quality of vision at the road level.

For motorized traffic, the European standards for road lighting (EN 13201 series [33,34,36,37]) consider the road luminance level as the key parameter for obtaining adequate vision conditions and traffic safety. The technical report 115 [38] of International Lighting Commission (CIE) adopts the same concept, while the USA standard RP-8-14 [39] focuses on the road surface luminance requirements between the proposed design possibilities.

During night and at the lighting levels that road lighting standards specify, the eye is adapted under the mesopic conditions. Under these conditions, the spectral distribution of the radiation reflected by the road surface to reach the driver's eyes influences his/her perception of brightness. Photometric instruments, calibrated under photopic conditions (i.e., at the lighting level of daylight eye adaptation), are not able to correctly quantify the real conditions as they measure the photopic lighting level (luminance). Only some national standards (Italy and UK) [40,41] and international guidelines [38] acknowledge and reference mesopic conditions [42].

In some conditions, such as for the evaluation of glare due to the lighting installation, the standards consider that the road luminance is also important for pedestrians [34], although it needs to be evaluated in a different view, as explained hereafter.

The road luminance is directly related to the direction of the incident luminous flux, the direction of view and the reflection characteristics of the road surfaces.

Road lighting standards conventionally consider the angle of observation of the road surface  $\alpha$  to be constant and equal to  $1^\circ$  [34], which is equivalent to a driver (with eyes at a height of 1.5 m above the road) seeing a portion of the road at a distance of about 87 m. Under this geometrical condition, luminance coefficient  $q$  (or the reduced luminance coefficient  $r$ ).

According to the angular convention adopted in EU standards, the luminance coefficient can be written as:

$$q(\alpha, \varepsilon, \beta) = \frac{L(\alpha, \beta + \frac{\pi}{2})}{E(\varepsilon, \beta)}, \quad (1)$$

where  $q(\alpha, \beta, \varepsilon)$  is the luminance coefficient of an elementary surface of the road considering the incident light path with angular coordinates  $(\varepsilon, \beta)$  and the viewing direction with angular coordinates  $(\alpha, \beta + \pi/2)$ , in reciprocal steradians;  $L(\alpha, \beta + \pi/2)$  is the luminance of the lighted elementary road surface when the viewing direction has angular coordinates  $(\alpha, \beta + \pi/2)$ , in candelas per square meter;

$E(\epsilon, \beta)$  is the illuminance on the lighted elementary road surface considering the incident light path with angular coordinates  $(\epsilon, \beta)$ , in lux;  $\alpha$  is the angle of observation of the point on road surface measured from the road surface, in degrees;  $\epsilon$  is the angle of incidence, which is the angle between the light path at the observed point on the road surface and the normal to this surface, in degrees; and  $\beta$  is the angle of deviation between the oriented vertical planes through the observer to the point of observation and from the point of observation through the luminaire, in degrees.

A scheme of the above angles is presented in Figure 1 for clarity of explanation. According to the assumption of the observation angle of the road surface  $\alpha$  being equal to  $1^\circ$ , the relevant standard introduces the reduced luminance coefficient  $r(\epsilon, \beta)$  for lighting installations, which is given by:

$$r(\epsilon, \beta) = q(\epsilon, \beta) \cos^3 \epsilon, \tag{2}$$

where  $r(\epsilon, \beta)$  is the luminance at the point, in candelas per square meter; and  $q(\epsilon, \beta)$  is the luminance coefficient of the elementary road surface for the incident light path with angular coordinates  $(\epsilon, \beta)$  and for the view direction with angular coordinates  $(\alpha = 1, \beta + \pi/2)$ , in reciprocal steradians.

To compare the brightness of road surfaces when lighted under the same conditions and considering the typical layouts of road lighting installations, the average luminance coefficient  $Q_0$  was introduced in a previous study [39]. It is defined by:

$$Q_0 = \frac{1}{\Omega} \int_{\Omega} q d\omega, \tag{3}$$

where  $\Omega$  is the solid angle defined by a rectangle parallel to the road surface at a height  $h$  equal to the height of the installed luminaries. To the reference point of the road surface, the rectangle is  $3 h$  wide with a length of  $4 h$  in the direction of travel and  $12 h$  in the opposite direction (Figure 2).

The reference values of the luminance coefficient  $q$  and  $Q_0$  are provided in CIE [43] and national standards, although they are more than 40 years old and do not consider coated road surfaces. For example, the Italian standard suggests the following values:  $Q_0 = 0.07$  for asphaltic pavements and  $Q_0 = 0.10$  for concrete pavements [40].

For pedestrians, the angles of observation of the road surface cannot be specified conventionally, but when  $\alpha$  is greater than  $10^\circ$ , the road surface works as a Lambertian surface and is characterized using the average diffuse reflectance. If measured data are not available, the European standard suggests  $\rho = 0.2$  as the default value [34].

- $\beta$  Deviation angle
- $\epsilon$  Incidence angle
- $\alpha$  Observation angle
- 1 Light Source
- 2 Light Direction
- 3 Observer

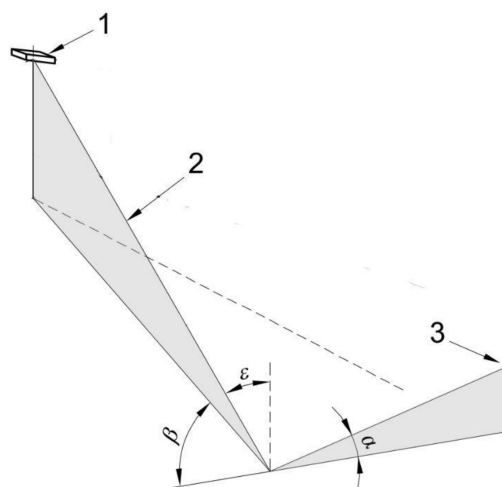
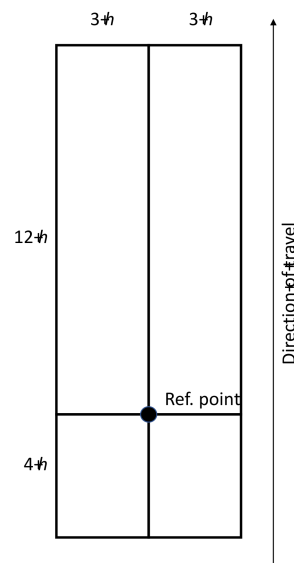


Figure 1. Relevant angles in the assessment of road lighting performances.



**Figure 2.** Dimension of the boundary area for  $Q_0$  calculation where  $h$  is the installation height of the luminaire.

## 2.2. Sample and Test Field Preparation

Table 1 describes the sample identification and measurement conditions used in this research. Two products were identified and implemented for this study: a grey and an off-white elastomeric coating. The two coatings were manually applied on an old smooth asphaltic road (Figure 3) within the INRIM (Istituto Nazionale di Ricerca Metrologica) premises and compared with the untreated adjacent road surface. The test site was divided in three different parts (Figure 3):

- R\_u:  $4 \times 10$  m of road untreated surface ( $40 \text{ m}^2$ );
- R\_g:  $4 \times 10$  m of road treated with grey coating ( $40 \text{ m}^2$ );
- R\_w:  $4 \times 4$  m of road treated with off-white coating ( $16 \text{ m}^2$ ).

Two asphaltic cores with a diameter of 150 mm were partially painted with the two coatings to obtain samples for laboratory characterization (Figure 4). The main difference between the two cores, which were named C1 and C2, is the texture of their surfaces, which depends on the characteristics of the asphaltic substrate. The purpose of this research is the measurement of optical properties of the materials in real working environments. The samples cores were useful for carrying out peculiar characterizations that are not possible with the portable instruments on site.

**Table 1.** Samples and measurement conditions.

Sample		Type	Code	Description	Measurements	Figure
Road	R	Smooth old road	R_u	Untreated	On site	3
			R_g	With grey coating		
			R_w	With off-white coating		
Core 1	C1	Smooth asphaltic	C1_u	Untreated	Laboratory	4a
			C1_g	With grey coating		
			C1_w	With off-white coating		
Core 2	C2	Rough asphaltic	C2_u	Untreated	Laboratory	4b
			C2_g	With grey coating		
			C2_w	With off-white coating		



**Figure 3.** View of the experimental installation, taken in condition of glazing sun lighting quite parallel to the direction of view to emphasize the different behavior of the actual asphalt and coated pavements (from top to bottom: actual asphalt, grey and off-white elastomeric coatings).

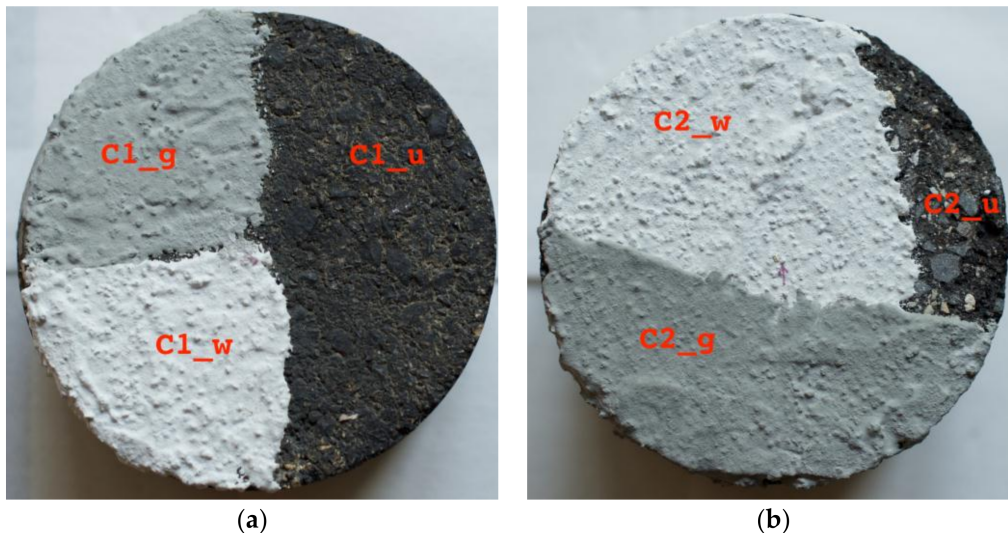


**Figure 4.** The two asphaltic cores used for laboratory testing (a) core 1; and (b) core 2.

### 2.3. Measured Quantities

The selected samples have been characterized in the laboratory and on site to assess their thermal and optical properties under different environment conditions. With reference to Table 1, the following quantities were measured for the listed samples:

- spectral reflectance in the solar range  $\rho_e$  of 300–2500 nm (C1, C2);
- spectral reflectance in the visible range  $\rho_v$  of 380–780 nm (C1, C2, R);
- chromaticity coordinates in different geometries (C1, C2, R);
- $q$  and  $r$  coefficients in standard required geometries (R); and
- thermal behavior (C1, C2, R).

#### 2.3.1. Optical and Luminous Characterization

The spectral optical properties, spectral reflectance and chromaticity coordinates of the three pavement typologies were measured in the laboratory with a double beam spectrophotometer Lambda 950 by Perkin Elmer, which was equipped with a 150 mm diameter Spectralon coated integrating sphere by Labsphere. The sphere accessory is needed for measuring the optical properties of scattering materials. Measurements were carried out for the whole solar spectrum of 300–2500 nm with an

angle of incidence of  $8^\circ$  and considering all the diffuse radiation (8/d geometry, specular component included). The spectral resolution was 1 nm and the absolute expanded measurement uncertainty was  $\pm 0.01$ . The slit aperture was set to 1 nm in the visible range and in servo mode in the near-infrared range. In this modality, the slit size changes according to the optimal energy input. Broadband values in the visible (v) and solar (e) range were calculated according to a previous study [44]. Visible quantities are calculated using the CIE standard Illuminant A as the reference incident source.

Chromaticity and reflection properties of the samples were also measured both in the laboratory and on site using a calibrated Hunter Lab MiniScan EZ4500 spectrophotometer with a spectral resolution and bandwidth of 10 nm. The instrument has a  $45^\circ/0^\circ$  geometry with a directional annular  $45^\circ$  illumination and a  $0^\circ$  viewing (specular components excluded). The absolute expanded measurement uncertainty of reflectance was  $\pm 0.08$  and the absolute expanded measurement uncertainty of the chromaticity coordinates in the CIE 1931 standard colorimetric system was  $\pm 0.005$ . The on-site measurement was carried out on a 1-m grid of measurement points to verify the homogeneity of the implementation carried out with hand tools.

### 2.3.2. Luminance Coefficient

Directional measurements were carried out with an incandescent light source to simulate the illuminant CIE A and a Photo Research PR650 spectroradiometer. This instrument has a spectral resolution of 4 nm and bandwidth of 8 nm. To fulfil requirement of the viewing angle of the road surface needing to be equal to  $1^\circ$ , the instrument was set at a height of about 30 cm and a measuring distance of about 17 m from the road measured surface. The measured area was an ellipse with the longest axis of about 3 m, which was centered in the middle of the testing area. In this way, the measured  $q$  was the average value that includes the inhomogeneity of the road surface coating. The relative expanded measurement uncertainty of the luminance coefficient was  $\pm 2\%$  and the absolute expanded measurement uncertainty of the chromaticity coordinates in the CIE 1931 standard colorimetric system was  $\pm 0.005$ .

### 2.3.3. Thermal Characterization

Thermal measurements were carried out with a NEC G100 thermography camera calibrated at INRIM. A preliminary test was carried out in the laboratory to confirm that all samples have the same emissivity and to estimate the measurement uncertainty of field measurements.

The first field tests have been conducted in the morning (starting at 9:30 a.m.) of an autumn day with a clear sky (20 September) to consider the conditions of a low temperature ( $19^\circ\text{C}$ ) of the road surface and the absence of direct solar radiation. Under these conditions, the influence of the optical properties of the coating on the measured temperature is minimized. The second field tests were carried out in the afternoon (starting at 3:40 p.m.) to consider the conditions of a higher temperature ( $23^\circ\text{C}$ ) of the road surface due to more than four hours of direct solar irradiation. Under these condition, the influence of the coating optical properties on the measured temperature is maximized with respect to the climatic conditions and the road surface position.

## 2.4. Calculations

To compare the performances of the coated surfaces and the untreated surfaces, a reference road lighting installation was simulated using the measured values of  $q$  and the measured luminous intensity distribution of a LED commercial luminaire design for road lighting. The luminaire has a luminous flux of  $6150 \pm 70$  lm and a luminous efficacy of  $55 \pm 0.9$  lm  $\text{W}^{-1}$ .

To evaluate and compare the power saving performances of road lighting installations, the European standard [33] defined the power density indicator  $D_P$  and the annual energy consumption indicator  $D_E$ . The first quantifies the ability of a luminaire to light the road at the given level with the minimum consumption of energy and as a first approximation, can be considered to not be correlated with the road surface characteristics. For our aim, the second one is more interesting because it depends

on the road surface properties. For a simple installation, a single operation profile can be calculated with the following formula:

$$D_E = \frac{Pt}{A} \quad (4)$$

where  $P$  is the system power of the lighting installation used to light the relevant area, in watts;  $t$  is the duration of the operation profile when the power  $P$  is consumed over a year, in hours; and  $A$  is the size of the area lit by the lighting installation, in meters.

Following the European standard [33], a two-lane road for motorized traffic was considered. The carriageway has a width of 8 m, the distance between luminaires was 35 m with a height of 8 m. The design target was to obtain a M3 lighting class [40] (minimum maintained average road luminance of  $1 \text{ cd m}^{-2}$ , minimum overall uniformity of 0.4 and minimum longitudinal uniformity of 0.60) when considering a road surface of type C2 with  $Q_0 = 0.07$  [43] as the most common surface used by lighting engineers.

Considering the above described conditions, the European standard [33] provides the typical values of  $D_P = 27 \text{ mW lx}^{-1} \text{ m}^{-2}$  and  $D_E = 1.6 \text{ kWh m}^{-2}$  when a full power operational profile is adopted with an annual operation time equal to 4000 h.

### 3. Results

#### 3.1. Laboratory Characterisation

Figure 5 shows the spectral reflectance of the investigated materials, which was measured on the two cores (C1, C2 samples). Although the untreated surfaces show substantial differences both in the visible and in the IR ranges due to their different composition and mechanical structure (due to bitumen and different rocks dimensions as larger dimensions result in higher reflectance), the two coated surfaces show differences that are lower than the measurement uncertainty and surface homogeneity, with graphs that are similar to each other. From the spectral point of view, the coating masks the influence of optical properties of the substrate and of its mechanical characteristics. Thus, for a given coating, the main factor determining its on-site optical properties is the application technique.

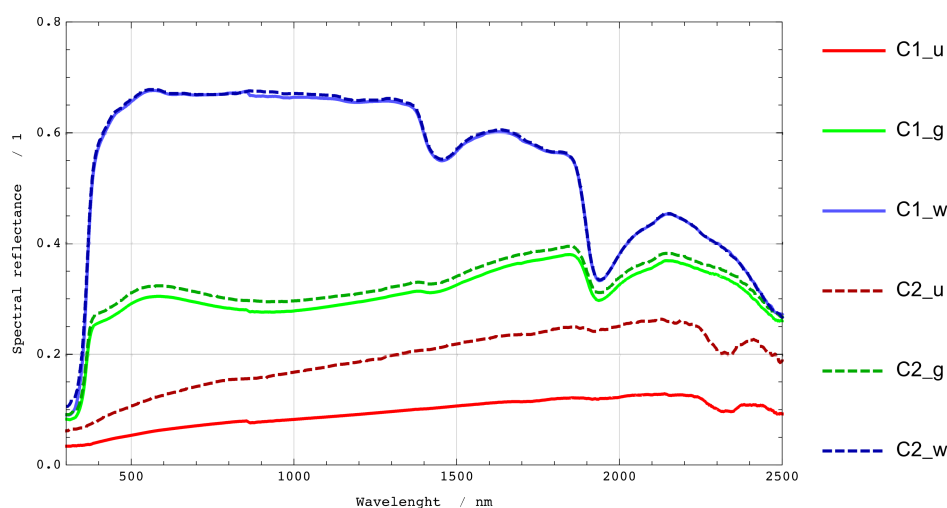


**Figure 5.** Spectral reflectance in the 300–2500 nm wavelength range of the cores (see Table 1) measured in laboratory conditions (8/d geometry).

With regards to the spectral response of the products, the grey coating (C1\_g and C2\_g) has a spectral reflectance of up to 1900 nm, while the reflectance of the off-white coating (C1\_w and C2\_w) starts decreasing at 1400 nm. The two coatings have practically the same behavior in the 1900–2500 nm range. The consequences of this behavior are highlighted in Figure 6 where the spectral distribution of

the solar radiation reflected by the different surfaces of the cores is shown. The differences between the grey and off-white coatings are small over 1900 nm but they become remarkable in the near infrared and visible ranges. In Table 2, the solar reflectance [45] and the luminous reflectance considering the CIE Standard Illuminant A and CIE Standard Illuminant D65 as incident sources are presented. This shows that the spectral distribution of the incident light does not influence the reflectance values. This aspect is important in road lighting where sources with different correlated color temperature and color rendering properties are used.

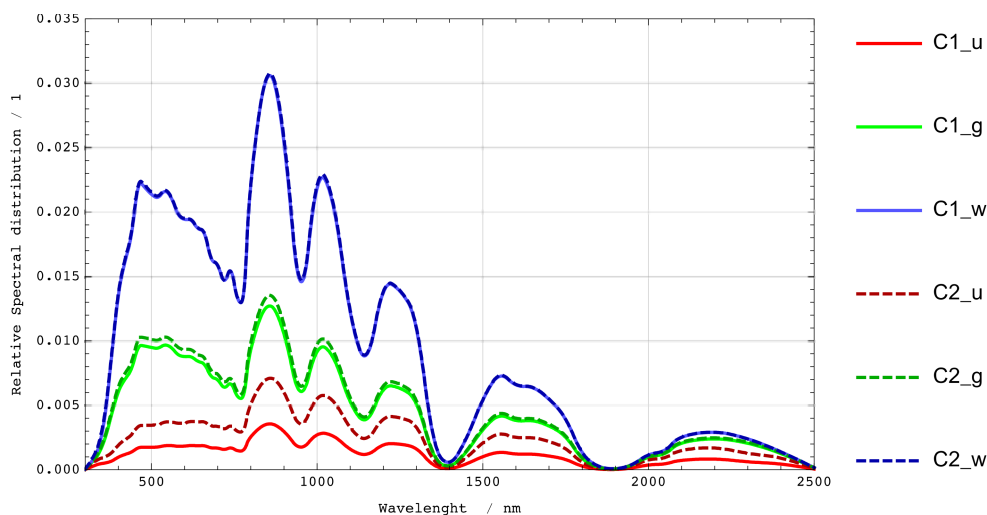


**Figure 6.** Spectral distribution in the 300–2500 nm wavelength range of the solar radiation reflected by the cores (see Table 1) considering the measured values of reflectance in laboratory conditions (8/d geometry).

**Table 2.** Solar reflectance  $\rho_e$  and luminous reflectance  $\rho_v$  of the two cores (see Table 1) measured in laboratory conditions (8/d geometry).

Sample	$\rho_e$	$\rho_v$ Ill. A	$\rho_v$ Ill. D65
C1_u	0.07	0.06	0.06
C1_g	0.29	0.30	0.30
C1_w	0.63	0.67	0.67
C2_u	0.14	0.12	0.12
C2_g	0.30	0.32	0.32
C2_w	0.63	0.67	0.67

The same behavior was found under different geometric measurement conditions, which is shown in Table 3. The measurements were carried out with two different instruments on a different measuring area. Considering the measurement uncertainty and the sample homogeneity, the CIE chromaticity coordinates and luminous reflectance are the same if the values of this quantity are slightly greater in the 45/0 geometry in the table. Colorimetric results refer to CIE Standard Illuminant A only for brevity.

Table 4 summarizes the influence of the azimuthal angle, which is essentially the effect of the surface texture and anisotropy with the incidence plane. In the geometrical conditions considered, similar to those usually observed for pedestrian traffic, the untreated surfaces show some moderate effects, while such effects are negligible for the cool coatings (off-white and grey). This difference depends on the influences of the mechanical structure and texture of the substrate, which are masked by the coatings.

**Table 3.** Luminous reflectance  $\rho_v$  and chromaticity coordinates  $x, y$  of the two cores considering different measurement geometries.

Sample	Measurement Conditions		$\rho_v$ (—)	$x$ (—)	$y$ (—)
	Incidence (°)	Observation (°)			
C1_u	45	0	0.07	0.47	0.41
	8	d	0.06	0.47	0.41
C1_g	45	0	0.30	0.46	0.42
	8	d	0.30	0.45	0.41
C1_w	0	45	0.76	0.45	0.41
	8	d	0.67	0.45	0.41
C2_u	45	0	0.14	0.46	0.41
	8	d	0.12	0.47	0.41
C2_g	45	0	0.32	0.45	0.41
	8	d	0.32	0.45	0.41
C2_w	0	45	0.69	0.45	0.41
	8	d	0.67	0.45	0.41

**Table 4.** Influence of the azimuthal angle on the reflectance of the analyzed products.

Sample	Measurement Conditions		$\rho_v$ Relative Change (%)			
	$\epsilon$ (°)	$\alpha$ (°)	$\beta$			
			0°	90°	180°	270°
C1_u	45	0	0	−1	5	3
C1_g	45	0	0	−2	−1	0
C1_w	45	0	0	0	0	−1
C2_u	45	0	0	2	5	4
C2_g	45	0	0	−1	0	0
C2_w	0	45	0	1	−1	−1

Considering the thermal properties, Figure 7 presents the false color thermal images of the two cores after 3 days of thermal stabilization in a temperature-controlled laboratory. These measurements show that treated and untreated cores have uniform surface temperatures. Negligible differences exist in the emissivity between the asphalt substrate and the two cool materials. In this sense, conventional and reflective materials have the same potential in cooling down by radiation at night.

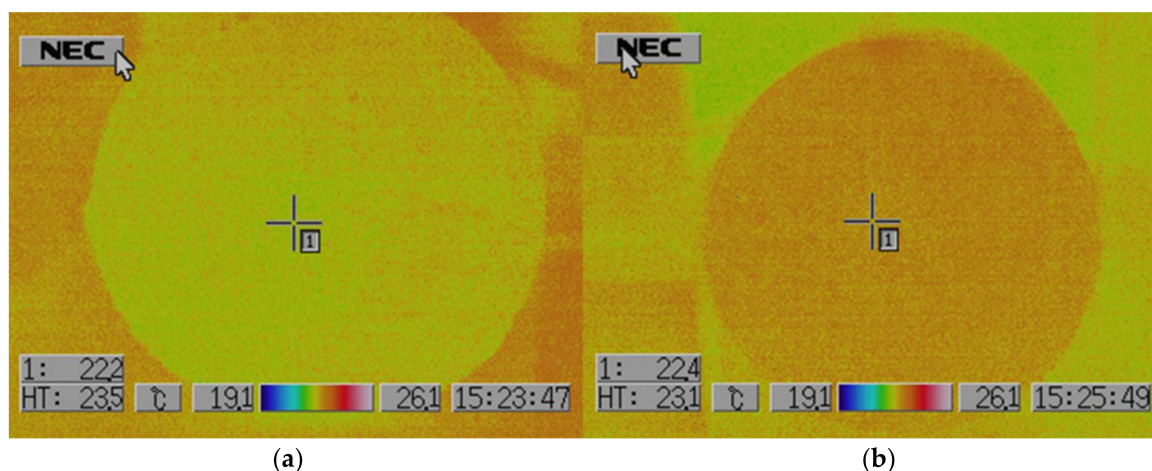


**Figure 7.** False color image of thermal measurement of (a) C1; and (b) C2.

### 3.2. On Field Characterisation

Considering the on-site measurements, the first step was to test the homogeneity of the coatings over the large treated surface area. The mean and the standard deviation of the measured values are reported in Table 5. The reflectance measurements have been carried out in the 45/0 geometry on several points in a grid with slots of 1 × 1 m. The low standard deviation demonstrated a good repeatability between the measured points and a good uniformity of the samples area. Visually, in typical motor traffic conditions (Figure 1), the homogeneity is not so good. However, under these measurement conditions, the measured area is large enough to give an average value useful for the design of the road lighting installation.

**Table 5.** On-site measurement of the homogeneity of the untreated and coated road surfaces. The measurements have been carried out on a grid of points as described in the text.

Sample	Value	$\rho_v$ (—)	x (—)	y (—)
R_u	Mean	0.12	0.468	0.415
	Standard deviation	0.01	0.006	0.001
R_g	Mean	0.33	0.461	0.414
	Standard deviation	0.03	0.009	0.002
R_w	Mean	0.64	0.453	0.412
	Standard deviation	0.01	0.002	0.001

Table 6 shows an example of the measured luminance coefficient  $q$  and the reduced luminance coefficient  $r$  for the standard measurement conditions in real urban environments. For comparison purposes, the tabulated values of a typical reference road (R\_s), used at the designing stage of road lighting installations, are shown. By increasing the angle of incidence  $\epsilon$ , the reduced luminance coefficient ( $r \cdot 10^4$ ) of the tested road (R\_u) has a greater decrement compared to the standard road R\_s. This can be explained by the conditions of the tested road, namely whether it is old and has deteriorated. On the other hand, it is important to note that the reduced luminance coefficient of the off-white surface (R\_w) is 1.5–4 times that of R\_s. The grey coating also significantly increases values of the design parameters. This aspect can be critical in retrofit works, since cool materials, characterized by a smoother surface, may severely affect the luminance uniformity of the lighted road. In practical terms, implementing this type of road surfaces needs the design and use of new luminaires, which are suitable for the peculiarities of these road coatings.

**Table 6.** Measured luminance coefficient and reduced luminance coefficient compared to the suggested values (R\_s) of a reference road generally adopted in the design of road lighting installations [41,44].

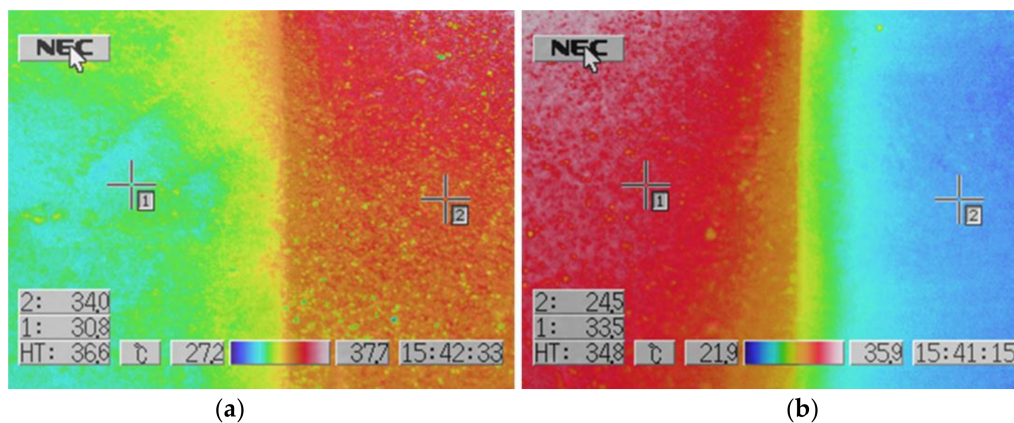
$\epsilon$	tan ( $\epsilon$ )	$\beta$	R_u		R_g		R_w		R_s	
			$q$	$r \cdot 10^4$						
(°)	(—)	(°)	( $sr^{-1}$ )	(—)						
30	0.57	0	0.059	380	0.121	789	0.235	1527	0.058	379
35	0.70	0	0.064	350	0.107	589	0.215	1183	0.069	380
40	0.84	0	0.073	330	0.101	456	0.153	687	0.084	377
45	1.00	0	0.091	320	0.121	429	0.146	516	0.105	372

Table 7 presents the effect of the luminance coefficient  $q$  for different observation and radiation incidence angles on the selected materials. The table also shows the relative change  $\Delta q$  of the cool materials with respect to the untreated asphaltic road R\_u. At high observation angles, the cool materials show Lambertian diffusing behavior for pedestrian traffic. At the same time, the reflected radiation increases with an increase in the  $\alpha$  angle. This implies that the installed power of road lighting system should be adequately reduced in the case of using reflective coating to avoid excessive lighting levels and lighting pollution. In this sense, the ratio  $Q_0 (\alpha = 1^\circ)/Q_0 (\alpha = 45^\circ)$  could be proposed as an indicator of the coating performances for the luminous pollution control.

**Table 7.** On-site characterization of the road surfaces considering geometric conditions of incidence and observation typical of pedestrian traffic.

Observation	Incidence	R <sub>g</sub>		R <sub>w</sub>		R <sub>u</sub>
$\alpha$ (°)	$\varepsilon$ (°)	$q$ (sr <sup>-1</sup> )	$\Delta q$ (%)	$q$ (sr <sup>-1</sup> )	$\Delta q$ (%)	$q$ (sr <sup>-1</sup> )
20	15	0.253	206	0.319	286	0.083
30		0.16	167	0.243	303	0.06
45		0.12	123	0.218	304	0.054
20	30	0.117	113	0.218	295	0.055
30		0.115	122	0.212	307	0.052
45		0.108	118	0.202	309	0.049
20	35	0.124	170	0.205	345	0.046
30		0.114	151	0.212	367	0.045
45		0.108	157	0.207	393	0.042
20	40	0.111	146	0.205	354	0.045
30		0.109	155	0.212	396	0.043
45		0.105	146	0.207	386	0.043
20	45	0.105	138	0.204	363	0.044
30		0.106	146	0.204	374	0.043
45		0.102	130	0.205	361	0.044

Thermal measurements were also carried out on site. Figure 8 presents the false color images acquired in the afternoon by the thermal camera of the actual asphalt, showing the grey coating (left) in addition to the off-white coating and the actual asphalt (right). The results, averaged across the whole area, are summarized in Table 8 and refer to the three pavement products. The results show the benefits of cool coating in reducing the surface temperature and thus, mitigating the urban environment. The strongest difference in thermal behavior between untreated road surface and off-white coated road surface was 9 °C during a day with clear sky and mild atmospheric temperatures. In the same conditions, the grey coating registered a surface temperature reduction of 3 °C.



**Figure 8.** False color image of thermal measurement on site of (a) R1<sub>u</sub> and R1<sub>g</sub>; (b) R1<sub>u</sub> and R1<sub>w</sub>.

**Table 8.** On-site surface temperature measurements in the morning and in the afternoon.

Measurement	R <sub>u</sub>		R <sub>g</sub>		R <sub>w</sub>	
	$T$	$T$	$T(u)-T(g)$	$T$	$T(u)-T(w)$	$T(g)-T(w)$
	(°C)	(°C)	(°C)	(°C)	(°C)	(°C)
Morning	19.8	19.9	-0.1	18.8	1	1.1
Afternoon	33.8	30.8	3	24.5	9.3	6.3

### 3.3. Energy Performances Results

The values of the annual energy use for road electric lighting  $D_E$  calculated for the three surfaces are presented in Table 9. In this table,  $\Delta D_E$  is the relative percentage change of  $D_E$  between the road lighting installation with the given coated surface and the untreated road surface. The results in this table consider only the luminance level and not the uniformity because it would require optimization of installation layout and luminous intensity distribution of luminaires, which is out of the scope of this research. Energy consumption can be strongly reduced using cool materials, although such results could be achieved only using properly designed installation. Furthermore, this takes into account the light scattering of cool and smoother products and the opposite object contrast on road surface. The pro/cons in using this type of coating on road surfaces is discussed in the conclusions in more detail, with consideration of the thermal impact and energy performances. Economic analyses have not been considered, but in case of a full feasibility study, the higher costs for pavements works, including periodic recoating, should be taken into account.

**Table 9.** Annual energy consumption indicator of the road lighting installation described in the text.

Sample	Energy Consumption	Energy Savings
	(kWh m <sup>-1</sup> )	(%)
R1_u	1.61	—
R1_g	0.52	67.5
R1_w	0.38	76.2

## 4. Discussion

The use of high reflective materials for road surfaces can reduce the UHI effect during the day and improve energy saving and traffic safety during night. Apart from the thermal aspects, high reflectance coating can reduce the energy consumption for roads or outdoor lighting installations. They can also improve visual perception of objects (obstacles) or pedestrians because of the opposite contrast against light background on the carriages and then increase road environment safety. Considering road lighting, it is possible:

- to reduce the installed luminous flux in addition to reaching the prescribed normative requirements about the road surface luminance;
- to improve the visual behavior due to the increased diffused part of the reflected light, with a consequent increase in the surrounding luminance with a reduction of glare (from lighting sources—luminaires) and improvement in the safety of pedestrians;
- to improve light pollution as a counter-effect, especially in extra-urban areas, where the diffused part of the reflected luminous flux would not be shielded by buildings as in the urban zone. This negative effect could be reduced or compensated optimization of the reflectance behavior in the specular directions. In this way, the reduction in the installed luminous flux could counterbalance the increment of the diffuse component of the light.

The introduction of high reflective and thus, brighter road surfaces would have strong influences in design and maintenance of road lighting installations and energy saving. However, for the large diffusion and application of this technology, at least three steps are necessary:

- the availability of reliable reference data of actual (or oncoming) high reflective coating materials, considering the influences of aging with time and maintenance;
- the strong control of the implementation techniques to guarantee repeatability of the optical properties of the coated road surface on the same site and between sites; and
- the development of luminaires with peculiar luminous intensity distributions to guarantee the normative requirements in the uniformity of the road surface luminance without changing the layout of road lighting installations, such as the inter-distance between consecutive columns.

The availability of reliable implementation techniques and reference data of current (or oncoming) high reflective coating materials will allow lighting designers to gather the energy savings and quality parameters forecasted in standards and meet the EU commitment to cut energy consumptions as committed by 2020 and 2030 Key Performances Target [46]. Thus, they will provide more efficient and safe road lighting for all users.

In a more general view, it can be observed that highly reflective coatings with reference to untreated road surfaces provide high potentials for thermal mitigation, with high energy savings for artificial lighting. However, they heavily affect the fraction of light scattered upwards, which is not useful for traffic safety. Grey and thus, moderately reflective coatings have a weaker impact on urban temperature than white coatings, but still provide relevant energy savings when road surfaces performances are considered with a viewing angle of 1° in road lighting calculations. Under this geometrical condition, the photometric performances of white and grey coatings are not significantly different, but grey has the advantage of being less disturbing to users. The trade-off between energy savings achievable by temperature mitigation and artificial lighting compared to the visual comfort for users is a crucial aspect that needs to be further explored, since few data are available yet. This topic will be addressed in the next phase of this research where different road surfaces painting techniques will also be considered.

**Acknowledgments:** Part of this work was funded by the Italian Ministry of Economic Development in the framework of the Program “RSE—Ricerca di Sistema Elettrico”. Part of this work is part of project “16NRM02 Surface, Pavement surface characterization for smart and efficient road lighting” that has received funding from the EMPIR program. EMPIR program is co-financed by the Participating States and from the European Union’s Horizon 2020 research and innovation program and funded the publishing fees.

**Author Contributions:** P.I., G.R. and M.Z. conceived and designed the experiments; P.I. performed the experiments; G.R. analyzed the data; M.Z. P.I. and G.R wrote the paper.

**Conflicts of Interest:** The authors declare no conflict of interest. The founding sponsors had no role in the design of the study; in the collection, analyses, or interpretation of data; in the writing of the manuscript, and in the decision to publish the results.

## References

- Oke, T.R. The energetic basis of the urban heat island. *Q. J. R. Meteorol. Soc.* **1982**, *108*, 1–24. [[CrossRef](#)]
- Oke, T.R. The urban energy balance. *Prog. Phys. Geogr.* **1988**, *12*, 471–508. [[CrossRef](#)]
- Taha, H. Urban climates and heat islands: Albedo, evapotranspiration and anthropogenic heat. *Energy Build.* **1997**, *25*, 99–103. [[CrossRef](#)]
- Akbari, H.; Davis, S.; Dorsano, S.; Huang, J.; Winert, S. *Cooling Our Communities Guidebook on Tree Planting and White Coloured Surfacing*; US Environmental Protection Agency, Office of Policy Analysis, Climate Change Division: Washington, DC, USA, 1992.
- Arnfield, A.J. Two decades of urban climate research: A review of turbulence, exchanges of energy and water, and the urban heat island. *Int. J. Climatol.* **2003**, *23*, 1–26. [[CrossRef](#)]
- Santamouris, M. *Energy and Climate in the Urban Built Environment*; James and James Science Publishers: London, UK, 2001.
- Akbari, H.; Kolokotsa, D. Three decades of urban heat islands and mitigation technologies research. *Energy Build.* **2016**, *133*, 834–842. [[CrossRef](#)]
- Akbari, H.; Rose, L.S. *Characterizing the Fabric of the Urban Environment: A Case Study of Salt Lake City, Utah*; LBNL-47851; Lawrence Berkeley National Laboratory: Berkeley, CA, USA, February 2001.
- Santamouris, M. Heat island research in Europe: The state of the art. *Adv. Build. Energy Res.* **2007**, *1*, 123–150. [[CrossRef](#)]
- Hirano, Y.; Fujita, T. Evaluation of the impact of the urban heat island on residential and commercial energy consumption in Tokyo. *Energy* **2012**, *37*, 371–383. [[CrossRef](#)]
- Santamouris, M.; Papanikolaou, N.; Livada, I.; Koronakis, I.; Georgakis, C.; Argiriou, A.; Assimakopoulos, D.N. On the impact of urban climate to the energy consumption of buildings. *Sol. Energy* **2001**, *70*, 3201–3216. [[CrossRef](#)]

12. Santamouris, M.; Paraponiaris, K.; Mihalakakou, G. Estimating the ecological footprint of the heat island effect over Athens, Greece. *Clim. Chang.* **2007**, *80*, 265–276. [[CrossRef](#)]
13. Sarrat, C.; Lemonsu, A.; Masson, V.; Guedalia, D. Impact of urban heat island on regional atmospheric pollution. *Atmos. Environ.* **2006**, *40*, 1743–1758. [[CrossRef](#)]
14. Santamouris, M.; Kolokotsa, D. On the impact of urban overheating and extreme climatic conditions on housing energy comfort and environmental quality of vulnerable population in Europe. *Energy Build.* **2015**, *98*, 125–133. [[CrossRef](#)]
15. Taleghani, M. Outdoor thermal comfort by different heat mitigation strategies—A review. *Renew. Sustain. Energy Rev.* **2018**, *81*, 2011–2018. [[CrossRef](#)]
16. Santamouris, M.; Ding, L.; Fiorito, F.; Oldfield, P.; Osmond, P.; Paolini, R.; Prasad, D.; Synnefa, A. Passive and active cooling for the outdoor built environment—Analysis and assessment of the cooling potential of mitigation technologies using performance data from 220 large scale projects. *Sol. Energy* **2017**, *154*, 14–33. [[CrossRef](#)]
17. Aflaki, A.; Mirmezahad, M.; Ghaffarianhoseini, A.; Ghaffarianhoseini, Z.; Omrany, H.; Akbari, H. Urban heat island mitigation strategies: A state-of-the-art review on Kuala Lumpur, Singapore and Hong Kong. *Cities* **2017**, *62*, 131–145. [[CrossRef](#)]
18. Gago, E.J.; Roldan, J.; Pacheco-Torres, R.; Ordóñez, J. The city and urban heat islands: A review of strategies to mitigate adverse effects. *Renew. Sustain. Energy Rev.* **2013**, *25*, 749–758. [[CrossRef](#)]
19. Zhai, J.; Previtali, J.M. Ancient vernacular architecture: Characteristics categorization and energy performance evaluation. *Energy Build.* **2010**, *42*, 357–365. [[CrossRef](#)]
20. Berdahl, P.; Bretz, S.E. Preliminary survey of the solar reflectance of cool roofing materials. *Energy Build.* **1997**, *25*, 149–158. [[CrossRef](#)]
21. Levinson, R.; Berdahl, P.; Akbari, H. Spectral solar optical properties of pigments Part II: Survey of common colorants. *Sol. Energy Mater. Sol. Cells* **2005**, *89*, 351–389. [[CrossRef](#)]
22. Synnefa, A.; Santamouri, M.; Apostolaki, K. On the development, optical properties and thermal performance of cool colored coatings for the urban environment. *Sol. Energy* **2007**, *81*, 488–497.
23. Synnefa, A.; Santamouris, M.; Livada, I. A study of the thermal performance and of reflective coatings for the urban environment. *Sol. Energy* **2006**, *80*, 968–981. [[CrossRef](#)]
24. Zinzi, M.; Agnoli, S. Cool and green roofs: An energy and comfort comparison between passive cooling and mitigation urban heat island techniques for residential buildings in the Mediterranean region. *Energy Build.* **2012**, *55*, 66–76. [[CrossRef](#)]
25. Santamouris, M. Using cool pavements as a mitigation strategy to fight urban heat island—A review of the actual developments. *Renew. Sustain. Energy Rev.* **2013**, *26*, 445–459. [[CrossRef](#)]
26. Qin, Y. A review on the development of cool pavements to mitigate urban heat island effect. *Renew. Sustain. Energy Rev.* **2015**, *52*, 445–459. [[CrossRef](#)]
27. Qin, Y. Urban canyon albedo and its implication on the use of reflective cool pavements. *Energy Build.* **2015**, *96*, 86–94. [[CrossRef](#)]
28. Mohajerani, A.; Bakaric, J.; Jeffrey-Bailey, T. The urban heat island effect, its causes, and mitigation, with reference to the thermal properties of asphalt concrete. *J. Environ. Manag.* **2017**, *197*, 522–538. [[CrossRef](#)] [[PubMed](#)]
29. Fintikakis, N.; Gaitani, N.; Santamouris, M.; Assimakopoulos, M.; Assimakopoulos, D.N.; Fintikaki, M.; Albanis, G.; Papadimitriou, K.; Chryssochoides, E.; Katopodi, K.; et al. Bioclimatic design of open public spaces in the historic centre of Tirana, Albania. *Sustain. Cities Soc.* **2011**, *1*, 54–62. [[CrossRef](#)]
30. Santamouris, M.; Xirafi, F.; Gaitani, N.; Spanou, A.; Saliari, M.; Vassilakopoulou, K. Improving the microclimate in a dense urban area using experimental and theoretical techniques. The case of Marousi, Athens. *Int. J. Ventilation* **2012**, *11*, 1–16. [[CrossRef](#)]
31. Shahidan, M.F.; Jones, P.J.; Gwilliam, J.; Salleh, E. An evaluation of outdoor and building environment cooling achieved through combination modification of trees with ground materials. *Build. Environ.* **2012**, *58*, 245–257. [[CrossRef](#)]
32. Zinzi, M.; Carnielo, E.; Rossi, G. Directional and angular response of construction materials solar properties: Characterisation and assessment. *Sol. Energy* **2015**, *115*, 52–67. [[CrossRef](#)]
33. CEN. *Road Lighting-Part 5: Energy Performance Indicators*; EN 13201-5:2015; CEN: Brussels, Belgium, 2015.
34. CEN. *Road Lighting-Part 3: Calculation of Performance*; EN 13201-3:2015; CEN: Brussels, Belgium, 2015.

35. Rossi, G.; Iacomussi, P.; Mancinelli, A.; DiLecce, P. Adaptive Systems in Road Lighting Installations. In Proceedings of the 28th Session of the CIE, Manchester, UK, 28 June–4 July 2015.
36. CEN. *Road Lighting-Part 2: Performance Requirements*; EN 13201-2:2015; CEN: Brussels, Belgium, 2015.
37. CEN. *Road Lighting-Part 4: Methods of Measuring Lighting Performance*; EN 13201-4:2015; CEN: Brussels, Belgium, 2015.
38. CIE. *Lighting of Roads for Motor and Pedestrian Traffic*, 2nd ed.; CIE 115:2010; CIE: Vienna, Austria, 2010.
39. Illuminating Engineering Society. *ANSI/IES RP-8-14:2014 Roadway Lighting*; Illuminating Engineering Society: New York, NY, USA, 2014.
40. UNI. *Illuminazione Stradale-Selezione Delle Categorie Illuminotecniche (Road Lighting-Selection of Lighting Classes)*; UNI 11248:2017; UNI: Milano, Italy, 2016.
41. BSI. *BS 5489-1:2013 Code of Practice for the Design of Road Lighting Part 1: Lighting of Roads and Public Amenity Areas*; BSI: London, UK, 2012.
42. CIE. *Recommended System for Mesopic Photometry Based on Visual Performance*; CIE 191:2010; CIE: Vienna, Austria, 2010.
43. CIE. *Road Surface and Road Marking Reflection Characteristic*; CIE 144:2001; CIE: Vienna, Austria, 2001.
44. CIE. *The Effect of Spectral Power Distribution on Lighting for Urban and Pedestrian Areas*; CIE 206:2014; CIE: Vienna, Austria, 2014.
45. ISO. *Glass in Building-Determination of Light Transmittance, Solar Direct Transmittance, Total Solar Energy Transmittance, Ultraviolet Transmittance and Related Glazing Factors*; ISO 9050, 2003; ISO: Geneva, Switzerland, 2003.
46. Available online: [http://ec.europa.eu/eurostat/statistics-explained/index.php/Europe\\_2020\\_indicators\\_-\\_background](http://ec.europa.eu/eurostat/statistics-explained/index.php/Europe_2020_indicators_-_background) (accessed on 4 March 2018).



© 2018 by the authors. Licensee MDPI, Basel, Switzerland. This article is an open access article distributed under the terms and conditions of the Creative Commons Attribution (CC BY) license (<http://creativecommons.org/licenses/by/4.0/>).